Vinculin-deficient PC12 Cell Lines Extend Unstable Lamellipodia and Filopodia and Have a Reduced Rate of Neurite Outgrowth

Barbara Varnum-Finney and Louis F. Reichardt

Department of Physiology, Howard Hughes Medical Institute, University of California, San Francisco, California 94143

Abstract. We have studied the role of vinculin in regulating integrin-dependent neurite outgrowth in PC12 cells, a neuronal cell line. Vinculin is a cytoskeletal protein believed to mediate interactions between integrins and the actin cytoskeleton. In differentiated PC12 cells, the cell body, the neurite, and the growth cone contain vinculin. Within the growth cone, both the proximal region of "consolidation" and the more distal region consisting of lamellipodia and filopodia contain vinculin.

To study the role of vinculin in neurite outgrowth, we generated vinculin-deficient isolates of PC12 cell lines by transfection with vectors expressing antisense vinculin RNA. In some of these cell lines, vinculin levels were reduced to 18–23% of normal levels. In the vinculin-deficient cell lines, neurite outgrowth on laminin was significantly reduced. In time-lapse analysis, growth cones advanced much more slowly than normal. Further analysis indicated that this deficit could be explained in large part by changes in the behaviors of filopodia and lamellipodia. Filopodia were formed in normal numbers, extended at normal rates, and extended to approximately normal lengths, but were much less stable in the vinculin deficient compared to control PC12 cells. Similarly, lamellipodia formed and grew nearly normally, but were dramatically less stable in the vinculin-deficient cells. This can account for the reduction in rate of growth cone advance. These results indicate that interactions between integrins and the actin-based cytoskeleton are necessary for stability of both filopodia and lamellipodia.

THE growth cone, the migratory tip of a growing axon, reproducibly follows a pathway for reaching a specific target during establishment of the embryonic nervous system. Filopodia and lamellipodia, dynamic elements located at the leading edge of a growth cone, extend and interact with chemotropic factors, extracellular matrix (ECM)[1] molecules, and neighboring cells. If a filopodium encounters a positive guidance cue, it persists and induces extension of the growth cone and axon towards the guidance cue (see e.g., O'Conner et al., 1990). If a filopodium does not encounter a guidance cue, it is eventually retracted and does not induce axon outgrowth. Hence, it has been suggested that filopodia serve as sensory antenna for the growth cone by establishing differential contacts in response to cues associated with nearby substrates and by subsequently directing axonal growth along appropriate pathways (for review see Bentley and O'Connor, 1994).

Please address all correspondence to Dr. Barbara Varnum-Finney, Department of Physiology, Howard Hughes Medical Institute, University of California, San Francisco, CA 94143-0724. Telephone: (415) 476-3976; FAX: (415) 566-4969.

1. *Abbreviation used in this paper*: ECM, extracellular matrix molecule.

At this time, only a few of the molecular constituents that are involved in establishing differential contacts between a growth cone and its substrate are identified. In other cell types, in particular fibroblasts, many of the proteins associated with close cell-substrate contacts, known as focal contacts, are identified (for review see Gumbiner, 1993). One of these proteins is the cytoskeletal molecule, vinculin (Geiger, 1979). In these contacts, vinculin is believed to function as a bridge between integrins, receptors for ECM molecules on the cell surface, and the F-actin cytoskeleton (for a recent review see Hynes, 1992). Vinculin associates directly with talin (Burridge and Mangeat, 1984) and α-actinin (Wachsstock et al., 1987) which are each believed to interact directly with integrins (Horwitz et al., 1986; Otey et al., 1990).

A direct correlation between levels of vinculin and number of focal contacts has been shown. In fibroblasts, reduction of vinculin protein levels by expression of antisense vinculin RNA results in a corresponding loss of focal contacts (Rodriguez Fernandez et al., 1993). An increase in vinculin protein levels by overexpression of vinculin RNA results in a corresponding increase in the number of focal contacts (Rodriguez Fernandez et al., 1992).

We directly address the role of vinculin in growth cone

motility in this report. Evidence suggests that vinculin might have a key role in establishing cell-substrate contacts in neurons. In several types of neurons and neuronal cell lines, vinculin is localized in the growth cone and branching regions of the neurite. These are regions of the neuron in close contact with the substrate (Halegoua, 1987; Letourneau and Shattuck, 1989). To directly assess the role of vinculin in growth cone motility, the amount of vinculin in PC12 cell lines was reduced by vectors expressing antisense vinculin RNA. This resulted in reduced growth cone advance rates which could be explained by decreased stability of filopodia and lamellipodia.

Materials and Methods

Cell Culture

PC12 cells were grown in standard culture flasks in Dulbecco's modified Eagle's medium with 4.5 g/liter glucose (DME H-21) supplemented with 10% heat-inactivated horse serum, 5.0% newborn calf serum, 2 mM glutamine, and 100 U/ml penicillin and streptomycin. The PC12 cells used in this study grow well attached to the tissue culture plastic as a dispersed monolayer (Tomaselli et al., 1987, 1990). Cells were passaged by incubating for 5–10 min with 0.5 mM EDTA in PBS (8 mM Na_2HPO_4, 2 mM KH_2PO_4, 2 mM KCl, 0.136 M NaCl, pH 7.4).

For priming with NGF, PC12 cells were passaged as described above onto fresh plates at a low density (10^4 cells/cm^2) and cultured for 5–7 d in DME H-21 supplemented with 1.0% heat-inactivated horse serum, 5.0% newborn calf serum, 2 mM glutamine, and 100 U/ml penicillin and streptomycin. In addition, 50 ng/ml NGF was added.

cDNA Cloning and Antisense Construction

A chicken cDNA, kindly provided by Dr. Susan Craig (Coutu and Craig, 1988), was used to screen a PC12 cDNA library provided by Drs. James Boulter and Stephen Heinemann (Salk Institute, La Jolla, CA) using a modified procedure of Maniatis et al. (1989) and Church and Gilbert (1984). Several positive clones were identified and shown to contain vinculin inserts by sequencing. The identity of these clones was verified by DNA sequencing. cDNA14, which contained 1.2 kb of the coding sequence and 300 bases 3′ to the stop codon, was used as an insert for the antisense experiments. This fragment was then subcloned in the antisense orientation in the retroviral expression vector LNCX (Miller and Rosman, 1989). Expression of the antisense vinculin cDNA was driven by the human cytomegalovirus (CMV) immediate early promoter. The vector containing insert was transfected by calcium phosphate coprecipitation (Graham and Van der Eb, 1973) into a packaging cell line, Psi2 cells (Mann et al., 1983). After selection in G418 (1 mg/ml), Psi2 culture medium containing viral particles was then used to infect high density PC12 cultures (2×10^5 cells/60-mm culture dish) in the presence of polybrene (10 μg/ml, Sigma Chem. Co., St. Louis, MO) for 4 h. PC12 cultures were then dissociated to single cells and replated at a low density (10^4 cells/60-mm culture dish), and after 2 d growth medium containing 1 mg/ml G418 was added. PC12 clones were then picked using cloning rings.

Cell Extracts

To obtain cell extracts for quantitating vinculin levels, PC12 cells were detached from tissue culture dishes with 0.5 mM EDTA (see above) and pelleted for 2 min in a microfuge (5,000 rpm). They were resuspended in an extraction buffer consisting of 50 mM Tris-HCl, pH 7.4, 1% Triton X-100, and 5 μg/ml each of chymostatin, leupeptin, aprotinin, pepstatin, and 1 mM PMSF. Extracts were rapidly pelleted at 10,000 rpm in a microfuge for 5 min to remove DNA, aliquoted, and frozen or used immediately. Total protein was determined for each extract using the Amido Schwartz method.

To obtain cell extracts of NGF-treated (primed) PC12 cells, PC12 cells were dissociated from culture substrates with 0.5 mM EDTA (see above) and replated in media containing 50 ng/ml NGF. Samples were then taken every 2 min. For blotting to detect MAP-kinase phosphorylation, cells were lysed with lysis buffer (0.1% Triton X-100, 50 mM Tris-HCl, pH 7.4, 150 mM NaCl, 2 mM EDTA and 5 μg/ml each of chymostatin, leupeptin, aprotinin, and pepstatin) containing 100 μM vanadate, and 1 mM DTT. For blotting to detect *c-fos* protein induction, cells were lysed with the above lysis buffer. Nuclei were removed from cell lysates by centrifugation at 2,000 rpm in the microfuge for 3 min. Supernatants were aliquoted and frozen or used immediately for antigen blotting.

Antigen Blotting

Extracts were mixed with electrophoresis sample buffer containing 3% beta-mercaptoethanol and boiled for 5 min. Samples were then run on 7% acrylamide gels with a 5% stack (Laemmli, 1970). For antigen blot analysis, proteins were electrophoretically transferred from gels to nitrocellulose filters (Schleicher and Schuell, Inc., Keene, NH) for 1 h at 500 mA. The filters were blocked in blocking buffer (5% Carnation nonfat dry milk in 100 mM Tris-HCl, pH 7.5, 150 mM NaCl, 0.5% NP-40) for 30 min. The filters were then incubated with 1 μg/ml of a monoclonal antibody to vinculin (Boehringer Mannheim, Indianapolis, IN, Cat. No. 1174843), tubulin (Sigma Chem. Co., St. Louis, MO, Cat. no. T-9026), or bovine phospholipase C, gamma-1 (PLC-γ-1, Upstate Biotechnology, Inc., Lake Placid, NY, Cat. no. 05-163). For chemiluminescence detection of antigens, blots were washed five times with blocking buffer and were then incubated for 30 min with peroxidase-conjugated anti-mouse IgG antibody (Cappel, Malvern, PA). Blots were washed five times with blocking buffer, once with the same solution without dry milk, and were then incubated with ECL reagents according to instructions with ECL kits (Amersham Corp., Arlington Heights, IL). Blots were placed next to film for 0.5 min–5 min to get a range of exposures.

Antigen blots were then analyzed with a densitometer and values for different exposures were plotted. An exposure in the linear range for the different clones was chosen for further analysis. Vinculin protein levels were normalized with both tubulin and PLC-γ-1 levels to control for differences in total protein loaded. A mean amount for control vinculin levels was calculated. Levels of vinculin from various control PC12 cell lines and cell lines expressing antisense vinculin RNA were then compared to the control mean.

To detect MAP-kinase, a mouse monoclonal diluted 1:5,000 was used (Zymed Labs., San Francisco, CA, Cat. No. 03-6600). To detect *c-fos*, a rabbit polyclonal antibody was used (Santa Cruz Biotechnology, Inc., Santa Cruz, CA, Cat. No. sc-52). For detection of proteins, blots were washed five times and then incubated for 30 min with alkaline phosphatase–conjugated anti-mouse or anti-rabbit IgG antibody, respectively (Promega, Madison, WI). They were then washed and phosphatase reaction product was generated by incubations at pH 9.5 with the substrates nitroblue tetrazolium (NBT) and 5-bromo-4-chloro-3-indolyl phosphate (BCIP, Sigma Chem. Co.).

Cell Attachment Assays

Cell attachment was measured as previously described by Tomaselli et al. (1987). Briefly, wells of 96-well Linbro Titertek plates (Flow Laboratories, McLean, VA) were coated with 80 μl laminin (10 μg/ml) solution diluted in PBS. Laminin was purified from Engelbreth-Holm-Swarm (EHS) sarcoma tumors using published procedures (Kleinman et al., 1982; Timpl et al., 1982). After overnight incubation at 4°C, wells were blocked for 3 h with 10 mg/ml solution of BSA (Sigma Chem. Co.). Wells were washed and 100 μl of a cell suspension (5×10^5 cells) in DME-H21 without serum was added. Plates were spun at 100 *g* for 1 min. Unattached cells were dislodged by pipetting 50 μl of DME-H21 down the sides of the wells. Detached cells were removed. The remaining cells were fixed and stained with a 0.5% crystal violet solution and solubilized with 1% SDS, and quantitated at A_{540} in a microtiter plate reader (Flow Laboratories).

Cell Preparation for Cell Staining, Neurite Outgrowth Assays, and Time-lapse Imaging

PC12 cells were primed with NGF for 5–6 d on a plastic substrate as previously described. Cells were then dissociated and replated as single cells into a well of 24-well culture dishes (Costar Corp., Cambridge, MA) containing a 12-mm Gold Seal coverslip for staining or into a well of a 6-well culture dish (Costar Corp.) containing a 22-mm Gold Seal coverslip for time-lapse imaging. Coverslips were previously coated with 1 mg/ml poly-ornithine (Sigma) for 15 min, after which they were extensively washed with water, and then coated with 10 μg/ml laminin overnight at 4°C. Cultures were incubated for one to two days in medium containing 50 ng/ml NGF in an 8% CO_2 atmosphere incubator maintained at 37°C.

Neurite Outgrowth Assays

Cells on coverslips were fixed with 4% paraformaldehyde and mounted on slides with gelvatol (50% glycerol plus Polyvinyl chloride). Cultures were viewed with an inverted Olympus IMT2 microscope with Nomarski optics. Microscope images were collected with a cooled CCD camera (Photometrics, series 200) equipped with a 1024 × 1024 pixel CCD imaging device (Texas Instruments, Tuscon, AZ, TC215) and stored on the hard disk in a VAX 3200 computer. Processes longer than 8 μm were measured using the Prism program (Chen et al., 1989).

To determine the percentage of cells with neurites, at least one hundred cells were analyzed per culture. The number of cells with a process longer than one cell diameter was determined and compared to the total number of cells counted.

Cell Staining

Coverslips were carefully transferred to a humidified staining chamber. Cells were fixed with 4% paraformaldehyde for 10 min, washed with PBS, and were then incubated with PBS containing 5% horse or donkey serum and 0.2% Triton X-100 for 10 min. Coverslips were then incubated overnight at 4°C with either a monoclonal antibody at 1 mg/ml or polyclonal antibody (1:200) to vinculin in PBS containing 5% horse or donkey serum. The monoclonal antibodies were purchased from Boehringer Mannheim (Indianapolis, IN) or from Sigma Chem. Co. The rabbit antiserum to vinculin was kindly provided by Dr. K. Burridge. Coverslips were then washed with PBS and coverslips previously treated with a monoclonal antibody were incubated with biotinylated horse anti-mouse IgG diluted 1:200 (Vector Laboratories, Burlingame, CA; Cat. No. BA-2001) for 30 min. The coverslips were then washed in PBS and incubated for 30 min with fluorescein-labeled streptavidin-fluorescein diluted 1:200 (Amersham Corp., Cat. No. RPN 1232). Coverslips previously treated with a polyclonal antibody were washed and incubated for 30 min with Texas-red labeled donkey anti-rabbit (Jackson Labs., Bar Harbor, ME, Cat. No. 711-075-132). Some coverslips were also incubated with rhodamine-labeled phalloidin diluted according to instructions (Molecular Probes, Eugene, OR, Cat. No. F-432). Coverslips were mounted on slides with gelvatol and viewed and photographed with a Nikon photomicroscope, using the appropriate filters.

Time-lapse Imaging of Growth Cones

Coverslips were carefully transferred to a viewing chamber containing DME H-21 (without phenol red) and 50 ng/ml NGF which was placed on the microscope for monitoring. This chamber was maintained at 37°C in a 95% O_2, 5% CO_2 atmosphere for the period of observation. Growth cones were allowed to adjust to this chamber for at least 15 min before viewing.

Growth cones were monitored with an inverted Olympus IMT2 microscope with Nomarski optics. Microscope images were collected with a cooled CCD camera (Photometrics, series 200) equipped with a 1024 × 1024 pixel CCD imaging device (Texas Instruments, TC215), stored on the hard disk in a VAX 3200 computer, and permanently archived onto 8-mm tape. Due to the high quality of the initial image, no image processing was necessary. To facilitate playback and data analysis, digital images were also converted to an analog format with a frame scan converter (Photron FSC-64000AL) and were then stored on optical disks using an optical disk recorder (Panasonic TQ-2026F). Short exposures (0.4 s) were taken at 6-s intervals for a 30-min period. Most growth cones remained very healthy for this period of time and those viewed longer were still healthy up to 90 min later when viewing was stopped.

Quantitation of Rate and Growth Cone Characteristics

Video images were played back using a disk recorder. For measuring the rates of growth cone movements, plastic sheets were placed over the video monitor and growth cone outlines were drawn at 5-min intervals. The centroid of the growth cone was estimated and the distance advanced (distance between centroids) determined for each time interval. The total distance advanced (the sum of each incremental advance) for the growth cone over the 30-min recording time was measured and a rate calculated. Rates for four to nine growth cones for each control or antisense cell line were determined.

For each of the same growth cones, the number of filopodia was determined every 5 min or four times during the recording period. A mean number of filopodia for each growth cone was determined from these counts. A mean of these means was determined for each PC12 clone and results are presented in Table II with a standard error of the mean (SEM). To measure filopodial extension rate, three to five filopodia from three to five of the same growth cones from each clone were followed. Due to difficulty in analyzing data, fewer growth cones were monitored for AS57 (n = 4) and for C3 (n = 3). The same growth cones were followed for D2 and AS9 as for all other characteristics. The location of the tip of each followed filopodium was determined at 6-s intervals. The following three periods of filopodial growth were observed: (*a*) a period of extension; (*b*) a period of nongrowth where the filopodia remained extended to the maximal length; and (*c*) a period of retraction. The rate of extension was determined from measurements made during the period of extension and the rate of retraction was determined from measurements made during the period of retraction.

To measure filopodial lifetime, five to ten filopodia were also followed from the first extension to the final retraction for each monitored growth cone. Generally, ten filopodia were followed from each growth cone, but for one growth cone from clone D2 and one from antisense 57, it was only possible to follow 5 filopodia. If possible for each growth cone, two filopodia extending approximately at angles of 0°, 45°, 90°, 135°, and 180° relative to the direction of growth were selected and monitored. Apart from selecting for the direction of extension, filopodia were chosen randomly. Each filopodium was followed from initial emergence from the growth cone

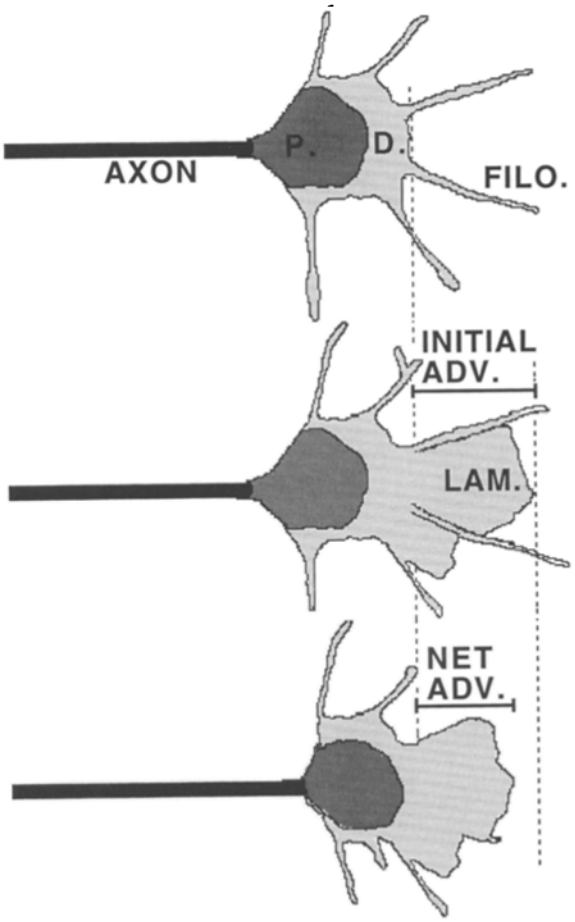

Figure 1. Cartoon depicting the growth cone regions and a single lamellipodial advance. A hypothetical growth cone with an axon, a proximal region (*P.*), and a distal region (*D.*) is seen extending filopodia (*FILO.*) and a lamellipodium (*LAM.*). The growth cone is shown at three different times during a lamellipodial growth cycle. The dashed line is drawn to indicate the location of the growth cone edge at the beginning and at the peak of the advance period. The first solid bar indicates the "Initial Adv." or distance that the lamellipodium has advanced before the quiescent period. The second bar indicates the "Net Adv." or the total distance that the lamellipodium advances during both the advance and quiescent periods (see Table II).

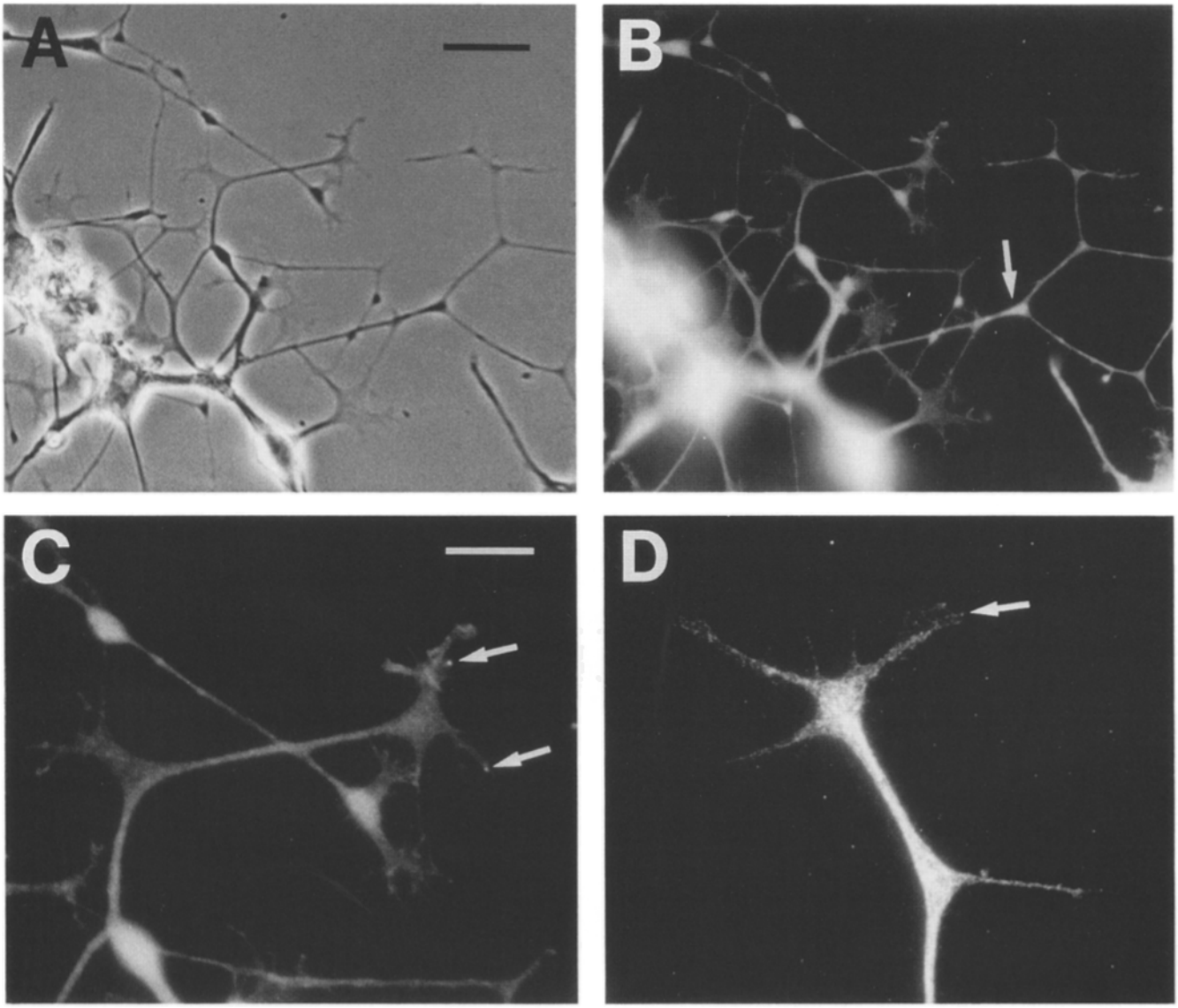

Figure 2. Localization of vinculin in primed control PC12 cells extending neurites on a laminin substrate. Cells grown on coverslips were fixed with paraformaldehyde, permeabilized with Triton X-100, and immunostained with a polyclonal anti-vinculin antibody followed by Texas-red labeled anti-rabbit IgG and viewed with phase microscopy (*A*) or with fluorescence using Texas-red filters (*B* and *C*) or with a monoclonal anti-vinculin antibody followed with fluorescein-labeled anti-mouse IgG (*D*). Vinculin was localized along neurites, at branch points, (*arrow in B*), lamellipodia, and at the tips of a subset of filopodia (*white arrows* in *C* and *D*). *A* and *B* are the same magnification. Bars: (*A*) 10 μm; (*C*) 20 μm. *C* and *D* are the same magnification.

edge to final retraction or engulfment by the advancing body of the growth cone. This time period was measured and referred to as the "Lifetime". A mean Lifetime for the five to twelve filopodia of each growth cone was determined. A mean of these means for four to ten (*n*) growth cones was determined for each PC12 cell clone and results are presented in Table II (±SEM). Additionally, the longest length that each filopodium attained was measured and similar statistics determined and presented in Table II as "Length".

To follow lamellipodia, a plastic sheet was again placed on the viewing screen and the outline of the lamellipodium drawn. The lifespan of each lamellipodium consisted of two characteristic periods. The first period was one of active growth. This was depicted as the " Advance Period" (Table III). The Advanced Period was the time from when a lamellipodium first formed at the growth cone edge until it stopped advancing. The second period was one of quiescence or retraction during which lamellipodia from control PC12 cell lines did not advance and occasionally retracted. This was depicted as the "Quiescent Period" (Table III). The Quiescent Period was the time from when the lamellipodium stopped advancing until the time of complete retraction or advance of a new lamellipodium. In addition, the distance that each lamellipodium advanced during the advance period was measured ("Initial Advance", Table III) and the net distance advanced during the advance and quiescent periods was also measured ("Net Advance", Table III). A cartoon describing these measurements is presented in Fig. 1. The advance period, quiescent period, initial advance, and net advance for each lamellipodium was determined and a mean of all advances for each growth cone was determined. A mean of the means for four to ten (*n*) growth cones was determined for each clone and presented in Table III (±SEM). Nested analysis of variance tests were performed for each of the measurements made (Sokol and Rohlf, 1969). Differences between means were considered significant if the *p* value was less than 0.05. Since the differences between

the means for all parameters were insignificant between control clones, D2 and C3, these were combined for statistical analysis. Since the differences between antisense clones AS9 and AS57 did not differ, these were also combined (Table III).

Results

Localization of Vinculin in PC12 Growth Cones

The major features of a PC12 growth cone include a region proximal to the neurite (designated *P.* in Fig. 1) and a region distal to the neurite (designated *D.* in Fig. 1). The region distal to the neurite consists of filopodia and lamellipodia whose behaviors are analyzed in this paper (see Fig. 1). To detect vinculin in PC12 growth cones, NGF responsive PC12 cells (primed, see Materials and Methods) extending neurites on a laminin substrate were fixed, permeabilized, and stained with either a polyclonal (Fig. 2, *B* and *C*) or a monoclonal (Fig. 2 *D*) antibody to vinculin (see Materials and Methods). Vinculin staining was observed in the cell body, the neurite, and the growth cone. Staining along the neurite was particularly bright at branch points (see *small arrow*, Fig. 2 *B*), although this may be due to an increased volume in this region. In the growth cone, punctate staining was observed in the region proximal to the neurite. This organelle rich region is closely attached to the substrate and is where consolidation is thought to occur (see e.g., Letourneau, 1979, 1983). Staining was also observed in the dynamic region distal to the neurite, consisting of filopodia or microspikes and the organelle free lamellipodia. Vinculin was localized along the entire length of the filopodium, and sometimes punctate staining appeared to be present at the filopodial tip (see *arrow*, Fig. 2, *C* and *D*). There was no staining over background levels when a non-specific polyclonal antibody or a monoclonal antibody of the same subtype was used (data not shown). Hence, the presence of vinculin in growth cones and in particular, its specific localization in lamellipodia and filopodia is consistent with a role for vinculin in establishing cell-substrate attachments in growth cones.

Antisense Expression of a Vinculin cDNA Results in Reduced Expression of Vinculin Protein

Two rat vinculin cDNAs were isolated from a PC12 library using a chicken vinculin cDNA as a probe. The identity of these clones was verified by DNA sequencing. cDNA14, which contained 1.2 kb of the coding sequence and 300 bases 3′ to the stop codon, was used as an insert for the antisense experiments. A packaging defective retroviral vector (LNCX) containing cDNA14 in the antisense orientation was used to infect PC12 cells. For controls, a retrovirus without cDNA inserts was used to infect cells. Infected cells were then selected for G418 resistance. Twenty antisense cell clones from two different infections and 10 control clones from two different infections were isolated.

To measure vinculin protein levels, lysates were prepared and proteins separated by polyacrylamide gel electrophoresis and immunoblotted with a monoclonal antibody raised against vinculin. As an initial screen, vinculin protein levels from antisense and control clones were visually compared. As would be expected, there was variability in vinculin levels among control clones. However, most antisense clones expressed lower levels of vinculin than the control clones that expressed the least amount of vinculin. In most antisense clones vinculin levels were reduced to between ~50–90% of control clone levels. Vinculin levels from two antisense clones, AS57 and AS9 from two different viral infections, were reproducibly reduced to ~18–30% of control clone levels. Four antisense clones were chosen for further quantitative analysis of vinculin levels. Two clones were chosen that expressed an intermediate amount of vinculin by visual analysis (AS34 and AS55) and two were chosen that expressed a much reduced amount (AS9 and AS57).

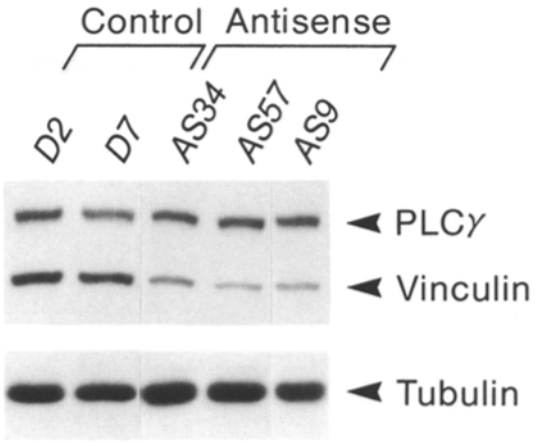

Figure 3. Antigen blot of cell extracts of PC12 clones transfected with the vector LNCX with or without an antisense cDNA insert. Equal amounts of total cell protein lysates from growing PC12 cells were separated by polyacrylamide electrophoresis and transferred to nitrocellulose. Vinculin protein was visualized by immunoblotting with a monoclonal antibody for vinculin followed by chemiluminescence detection with an anti-mouse IgG. To estimate total levels of protein in each lysate, two other proteins, PLC-gamma and tubulin, were also quantitated by antigen blot. Using densitometry, levels of vinculin were then normalized between clones using the PLC-γ and tubulin levels.

To quantitate protein levels, blots were analyzed with densitometry. In one blot, protein levels from seven control clones and three antisense clones were compared (selected control clone lanes and all antisense lanes are shown in Fig. 3 and protein levels normalized to the control mean level are shown in Table I). As expected the amount of vinculin expressed by the control clones was variable. For this blot, a mean control value was determined and normalized to 100. Normalized values for individual control clones were then calculated and these varied from 68–171% (±SD of 45%). Antisense clones expressed vinculin protein levels that were significantly reduced compared to the control clones. AS9 and AS57 expressed 23 and 18%, respectively, of the mean level of vinculin present in the seven control clones, and AS34 expressed ~40% of the mean level (Table I). Even when compared to the control clone expressing the least amount of vinculin, AS9 and AS57 expressed strikingly reduced levels of vinculin. Using analysis of variance tests, the mean level of protein expressed by the three antisense clones (AS34, AS9, and AS57) was significantly less than the mean level expressed by seven control clones ($p < 0.025$). In a sep-

Table I. Characterstics of Control and Vinculin-deficient Cell Lines

	Vinculin protein levels	Unprimed cell attachment	Primed cell attachment	Percent cells with neurites	Neurite length
					μm
Control					
D2	158	100	100	74 ± 6.7	91 ± 31.0
D7	172	–	–	85	93
Vinculin-deficient					
AS34	40	96	97 ± 3.0	64 ± 12.0	60 ± 2.5
AS55	–	–	–	67 ± 7.0	34 ± 6.1
AS9	23	–	80 ± 16	40 ± 11.0	25 ± 4.6
AS57	18	90	82 ± 19	51 ± 3.0	21 ± 1.5

Vinculin protein levels are from representative lanes of a single gel (Fig. 3). The blot was analyzed with densitometry and vinculin values were normalized for total protein using PLC-γ-1 and tubulin protein levels (see Materials and Methods). A mean vinculin protein value for seven control clones was determined. Values are a percentage of this mean value for each represented clone. Protein levels for AS55 were determined with a separate gel (see text). PC12 cell body attachment (see Materials and Methods) to substrates coated with 10 μg/ml laminin was measured for unprimed cells and for primed cells (incubated with NGF for 5–6 d as described in Materials and Methods). For each clone, the percentage of cells attached to laminin compared to poly-D-lysine was first determined and this value was normalized to control clone values. Unprimed attachment values are from a single representative experiment. Primed values are the mean from two experiments (±range). To determine the percent cells with neurites and neurite lengths, primed PC12 cells were replated as single cells into two wells of 24-well culture dishes containing a glass coverslip coated with 10 μg/ml laminin. After a 2-d incubation, cultures were fixed and coverslips were mounted onto slides. The percentage of cells with processes longer than one cell diameter for each culture (>100 cells counted) and a mean percentage for each clone (two cultures) was determined. A mean neurite length for each culture (20 neurites measured) and then a mean for each clone (two cultures) was determined. Values from D2, AS55, AS9, and AS57 are means of three experiments (±SD). Values from AS34 are means of two experiments (±range). Values from D7 are from a single representative experiment.

arate blot, clone AS57 expressed 29% of the mean level of vinculin present in two control clones and a fourth antisense clone, AS55, expressed 70% (blot not shown). Clearly, two antisense clones, AS9 and AS57, expressed significantly less vinculin than all control clones and two other clones, AS34 and AS55, expressed an intermediate amount of vinculin compared to control and the vinculin-deficient clones, AS9 and AS57.

Localization of Vinculin and Filamentous Actin in Antisense Cell Lines

To see whether reducing vinculin levels affected its cellular distribution, NGF-primed antisense (clone AS57) and control cells (clone D2) extending neurites on a laminin substrate were stained with a monoclonal antibody to vinculin (Fig. 4). In the antisense cells, staining for vinculin was very faint in both the cell body and the growth cone compared to staining in the control cells (compare Fig. 4, *A* and *C*). In contrast, phalloidin staining for filamentous actin was not detectably different in cells expressing normal or dramatically reduced levels of vinculin (compare Fig. 4, *B* and *D*), suggesting that actin localization does not depend on normal levels of vinculin.

Reduced Vinculin Expression Results in Shortened Neurites

PC12 cells from clones that expressed reduced levels of vinculin were capable of attaching to the plastic culture dishes and proliferated at a nearly normal rate (data not shown). In addition, proliferating cells from antisense clones AS34 and AS57 attached to a laminin substrate almost as well as cells from control clone D2 (see Table I). After priming for 5 d, attachment to laminin by cells from AS34 was not reduced and attachment by cells from clones AS9 and AS57 was only slightly reduced to ~80% of control values.

Although cell body attachment to a laminin substrate was only slightly reduced, cells from vinculin-deficient clones extended much shorter neurites than cells from control clones after priming and replating on a laminin substrate (Fig. 5). Neurites from clones AS9 and AS57, expressing the least amounts of vinculin were about 1/4 length of those from control clones, D2 and D7 (Fig. 5 and Table I). Neurites from two clones, AS34 and AS55, expressing an intermediate amount of vinculin, were also shortened and were on average about 66% and 37% the length of neurites from the control clones, respectively.

The reduced length of neurite extension was not due to the inability of these cells to respond to NGF, since about half of the cells from clones AS9 and AS57 were able to extend neurites of at least one cell diameter (see Table I). Also, addition of NGF to antisense clones resulted in normal responses on the molecular level. Addition of NGF to AS9 cells resulted in phosphorylation of MAP2 kinase with the same kinetics as seen in control clones (data not shown) and addition of NGF to clone AS57 cells induced the synthesis of c-FOS protein as shown by antigen blot analysis (data not shown).

Reduced Vinculin Expression Results in a Reduced Rate of Outgrowth and Unstable Filopodia and Lamellipodia

To address which growth cone characteristics are affected in vinculin reduced clones, growth cones migrating over a laminin substrate were monitored over a 20–30-min period using a CCD camera and computer system attached to an inverted microscope fitted with Nomarski optics as described (Materials and Methods). The characteristics analyzed included (*a*) the rate of growth cone migration, (*b*) the number, duration, and length of filopodial extensions, and (*c*) the length and type of lamellipodial extensions.

To insure that differences between control and antisense clones were due to differences in vinculin levels rather than other unrelated differences, growth cones from two different control clones and from several antisense clones were followed. Using analysis of variance, the means derived from measurements from the five cells from each of two indepen-

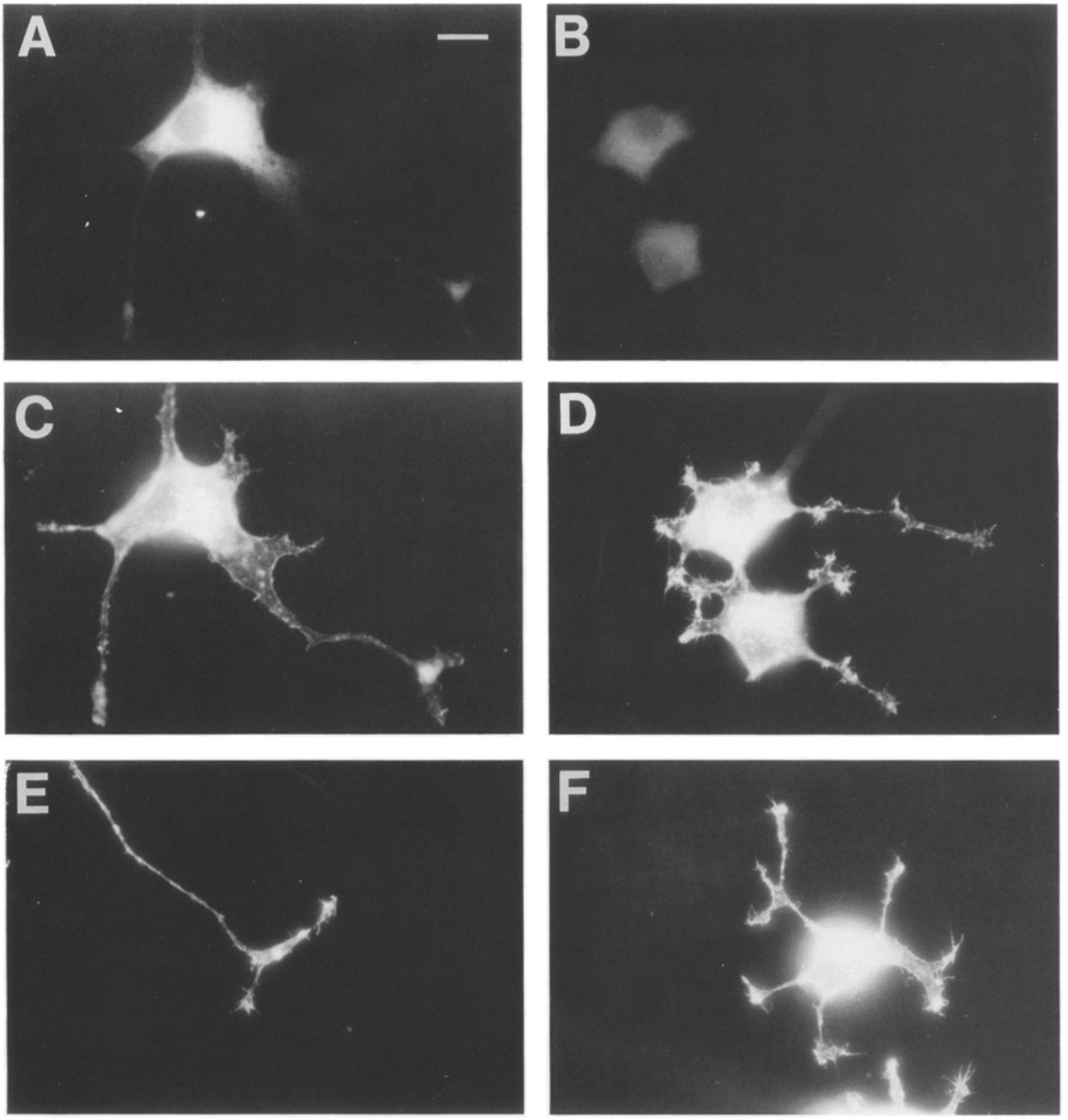

Figure 4. Localization of vinculin and actin filaments in primed PC12 cells extending neurites on a laminin substrate from control clone D2 antisense cell clone 57. Cells grown on coverslips were fixed with paraformaldehyde, permeabilized with Triton X-100, and stained with a monoclonal anti-vinculin antibody followed by fluorescein-labeled anti-mouse IgG and with rhodamine phalloidin. Specimens were then viewed with a fluorescence microscope using fluorescein (*A* and *B*) or rhodamine (*C–F*) filters and photographed using identical exposure times. (*A* and *C*) Cell from control clone D2 stained with anti-vinculin (*A*) and phalloidin (*C*); (*B* and *D*) cell from antisense clone 57 stained with anti-vinculin (*B*) and phalloidin (*D*); (*E*) growth cone from clone D2 stained with phalloidin; and (*F*) cell from antisense 57 stained with phalloidin. All micrographs are at the same magnification. Bar in *A* is 10 μm.

dently isolated control clones did not differ significantly. Therefore, for statistical comparisons to antisense cell lines, the means for the five cells from the two separate clones were combined for a total of ten cells. Also, using analysis of variance, the means derived from measurements of four cells of clone AS9 and 9 cells of AS57, the two antisense clones expressing a similarly reduced amount of vinculin, were not significantly different. Therefore for statistical comparisons to control cells, the means for the cells from the two separate clones were combined for a total of 13 cells (Table II).

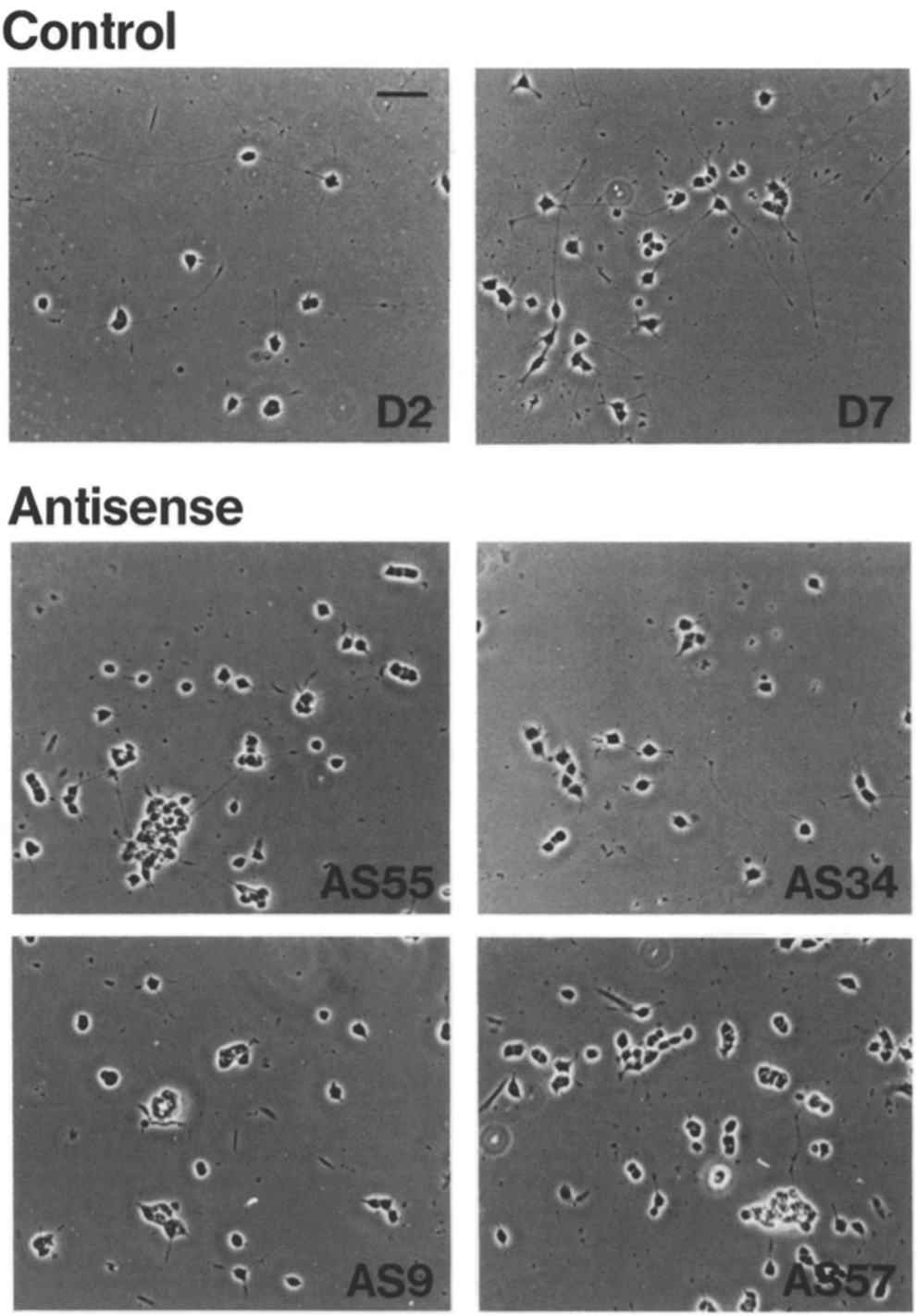

Figure 5. Neurite outgrowth by control and antisense cell lines. Primed PC12 cells were plated on laminin-coated coverslips and grown for 2 d, fixed, mounted, and viewed with phase contrast optics and photographed. All micrographs are at the same magnification. Bar in top left micrograph is 30 μm.

Rate of Growth Cone Migration. Results in Table II show that growth cones from cells expressing reduced levels of vinculin grew at a significantly reduced rate compared to the control clones. Those from antisense clones, AS9 and AS57, grew at ~30% the rate of the control clones, whereas one expressing an intermediate level of vinculin, AS55, grew at ~50% the normal rate (21.1 μm/h $\pm$ 8.5). The difference in growth rate between the combined antisense clones and combined control clones was very significant (Table II). These results strongly suggest that vinculin is involved in producing a maximal rate of outgrowth on a laminin substrate.

Filopodial Dynamics. To further characterize the effect of reduced vinculin levels on growth cones, filopodia were monitored in antisense and control clones of PC12 cells. Filopodia from control growth cones extended in all directions. Each growth cone extended between 1 and 14 filopodia at any one time. They varied in length from very short microspikes, the shortest being 1.5 μm, to as long as 12.5 μm. Individual filopodia usually remained in the same plane of focus with the growth cone edge, indicating they were probably attached to the substrate. Often filopodia remained like this for longer than three or four minutes (see *dark arrow*

Table II. Growth Cone Rate and Filopodial Characteristics

	Growth cone advance rate	Filopodia			
		Number	Lifetime	Extension rate	Length
	μm/h		*min*	*μm/s*	*μm*
Control					
D2 (n = 5)	54.2 ± 17.6	6.9 ± 2.0	4.3 ± 0.9	0.15 ± 0.01	5.6 ± 1.2
C3 (n =5)	40.2 ± 12.6	5.0 ± 0.6	4.1 ± 1.2	0.16 ± 0.03	5.1 ± 1.2
Combined means	47.2 ± 16.3	6.0 ± 1.7	4.2 ± 1.0	0.16 ± 0.02	5.4 ± 1.1
Vinculin-deficient					
AS9 (n = 4)	15.5 ± 3.4	2.3 ± 0.7	1.7 ± 0.2	0.15 ± 0.02	4.4 ± 0.5
AS57 (n = 9)	13.3 ± 6.2	2.9 ± 1.0	1.8 ± 0.4	0.14 ± 0.01	3.6 ± 0.9
Combined means	14.0 ± 5.5	2.8 ± 1.0	1.8 ± 0.4	0.15 ± 0.01	3.8 ± 0.8
p value	$p < 0.001$	$p < 0.001$	$p < 0.001$	NS*	$p < 0.01$

The growth cone advance rate was measured for each growth cone (see Materials and Methods). Values represent the mean for the number of growth cones (n) followed for each clone (±SD). Filopodial charcteristics were measured for the same growth cones (see Materials and Methods). The number of filopodia was counted at four different times during the recording period and a mean number for each growth cone was calculated. The mean number for each respective clone is given (±SEM). A mean extension rate, lifetime, and length for 5–10 filopodia from each growth cone was determined, and the mean for each clone is given (±SEM). A combined mean for control clones and a combined mean for vinculin-deficient clones is given (±SEM). p values were determined using analysis of variance comparing values from the combined clones.
* Not significant.

in Fig. 6 *A* at 150 s). Sometimes, filopodia detached from the substrate (see *dark arrow* at 0 s in Fig. 6 *A*). Eventually, many of the filopodia were retracted. However, filopodia extended in the same direction as a growing lamellipodium were often engulfed by the lamellipodium rather than being retracted (see *white arrow* at 0 s in Fig. 6 *A*). The engulfed filopodia often appeared to provide an infrastructure for lamellipodial growth.

Filopodia from antisense clones also extended in all directions. At any one time, there appeared to be fewer filopodia extended from these growth cones than from controls. In contrast to the control clones, very few filopodia remained in the same plane of focus as the growth cone edge. Instead, most filopodia detached from the substrate. Generally, antisense filopodia were retracted back into the growth cone sooner than control filopodia and were less likely to provide an infrastructure for lamellipodial growth. In addition, filopodia appeared somewhat shorter than the control filopodia. The number of short microspikes was greater in antisense clones than in control clones, the shortest one being 1.0 μm. Longer filopodial processes were also seen, the longest being 10 μm.

Four measurements were made to quantitate filopodial characteristics: (*a*) the number at any one time; (*b*) the rate of extension and retraction; (*c*) the lifetime; and (*d*) the length of filopodia. To determine the average number of filopodia extended by a growth cone at any one time, the number of filopodia was counted four different times during the viewing time and a mean number calculated for each growth cone. At any one time, the growth cones from the two antisense clones expressing the least amount of vinculin, AS9 and AS57, extended ~50% the number of filopodia compared to the growth cones from the control clones (Table II). The clone expressing an intermediate amount of vinculin, AS55, extended ~60% (3.5 ± 0.7). The data from the two control clones and the two antisense clones expressing comparably low amounts of vinculin, AS9 and AS57, were pooled and subjected to statistical analysis. The difference in the pooled means between the combined antisense and combined control clones was significant (see Table II).

To see whether vinculin-deficient growth cones initially extend fewer filopodia or whether the same numbers of filopodia were extended but were retracted sooner, the mean filopodial lifetime was determined. The average filopodial lifetime was determined by following five to ten randomly chosen filopodia from extension to retraction or engulfment for each growth cone. The mean filopodial lifetime was almost 60% shorter for the antisense clones AS9 and AS57 compared to the control clones (1.8 vs 4.2 min). The mean lifetime of a third antisense clone expressing an intermediate amount of vinculin, AS55, was ~50% shorter than the controls (2.2 min ± 0.9). The difference in the pooled means between the combined antisense and combined control clones was significant (see Table II). The distribution of filopodial lifetimes shows a general shift down in the normally distributed population mean for the antisense clones (Fig. 7 *B*). Interestingly, very few control filopodia had a lifetime shorter than 1 min (9%), but many antisense filopodia did (27%). In addition, a large number of control filopodia persisted longer than 4.0 min (40%), whereas very few antisense filopodia persisted this long (8%). The average rate of new filopodia formation can be calculated by dividing the average number observed by the average lifetime. Results suggest that ~1.4 and 1.5 filopodia per minute are formed in control and vinculin-deficient growth cones, respectively. This result demonstrates that very similar numbers of filopodia are initially extended from the antisense growth cones compared to the control growth cones. Also vinculin-deficient filopodia are extended at the same growth rate as control filopodia. However, after achieving a maximal length, vinculin-deficient filopodia are withdrawn sooner than control filopodia. Since they are withdrawn sooner, fewer filopodia are visible at any one time.

To further identify the defective characteristic in vinculin-deficient filopodia, the rate of filopodial extension and retraction were measured. Three periods during a filopo-

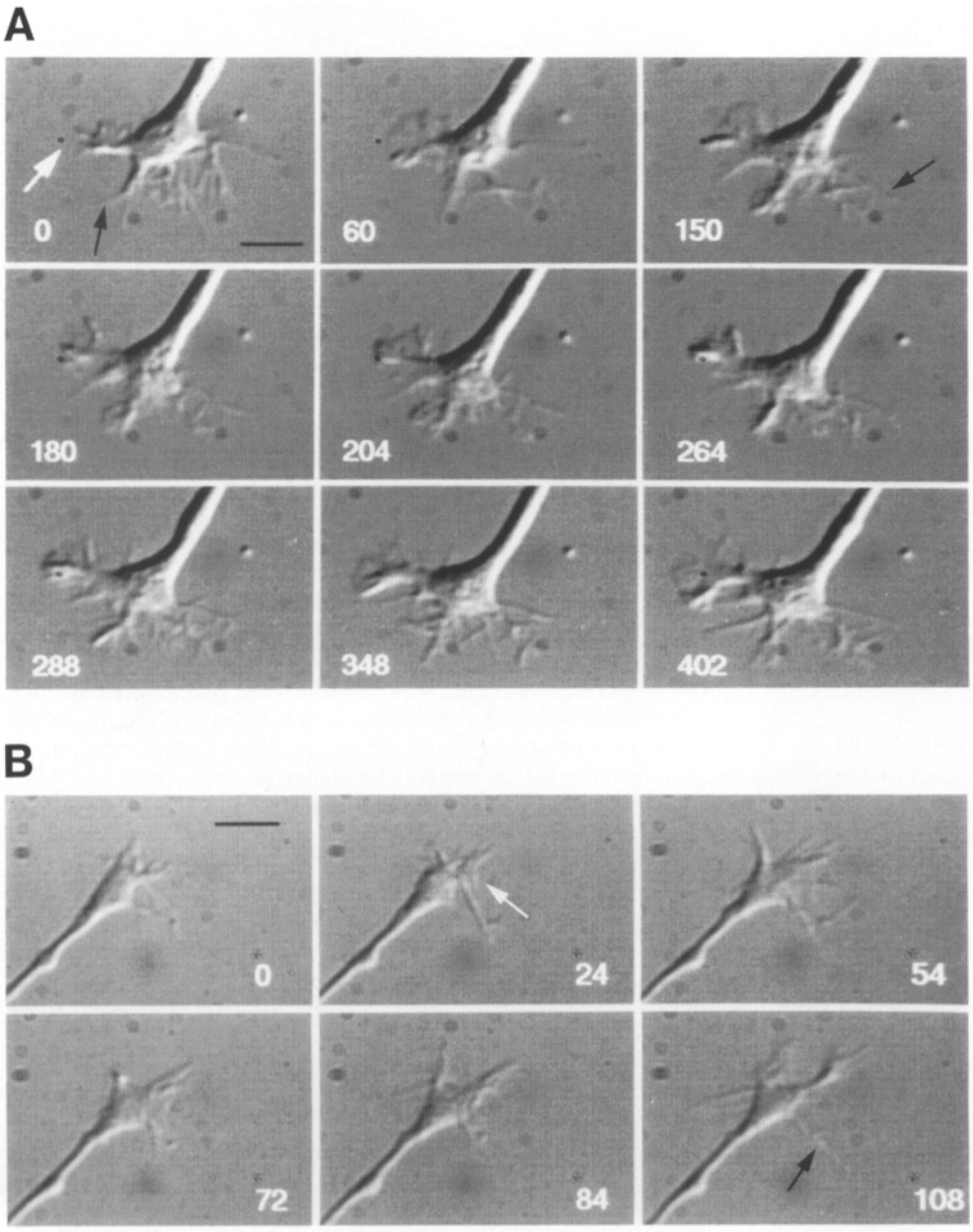

Figure 6. Representative growth cone from a control cell line, D2, and from an antisense cell line, AS57 depicted at different times to show growth cone characteristics. Primed cells from cell lines D2 and AS57 were plated on a laminin-coated glass coverslip and were monitored with an inverted microscope using Normarski optics. Images were collected every 6 s with a cooled CCD camera and stored on the hard disk of a Vax computer. Images from selected time points are shown (*white number* in the *bottom left corner* of each image represents the time in seconds of the image). (*A*) Representative growth cone from control line D2 depicting two periods of lamellipodial advance from 0 to 150 s and from 288 to 402 and a quiescent period from 180 to 264 s. The white arrow at 0 s indicates a short filopodium soon to be engulfed by an emerging lamellipodium. The dark arrow at 0 s indicates a filopodium detached from the substrate and waving in the growth medium. The dark arrow at 150 s indicates a filopodium which remains in the same plane of focus as the growth cone edge for longer than 4 min. (*B*) Representative growth cone from cell line AS57 depicting a period of lamellipodial advance from 0 to 54 s, and a quiescent period from 54 to 108 s. The white arrow at 24 s indicates an emerging lamellipodium. The dark arrow at 108 s represents an out of focus filopodium, waving in the culture medium. All micrographs are at the same magnification. Bars in top left micrographs of *A* and *B* are 5 μm.

dium's lifetime were observed: (*1*) a period of extension; (*2*) a period of nongrowth where the filopodium remained extended to the maximal length; and (*3*) a period of retraction. The filopodial extension rate was measured during the period of extension and the retraction rate was measured during the period of retraction. The rate of filopodial extension ranged from 0.1 to 0.3 μm/s. The average filopodial growth rate for each monitored growth cone was calculated from measurements made from five randomly chosen filopodia. The combined mean for the control clones was 0.16 μm/s (see Table II). The filopodial retraction rate was approximately the same as the extension rate and mean rates for extension and retraction did not differ significantly (data not shown). This result corroborates previously reported rates for filopodial extension and retraction (Sheetz et al., 1992). Interestingly, the mean filopodial extension rate was not significantly changed in vinculin-deficient clones (see Table II). The rate of retraction was likewise unaffected (data not shown).

The maximum length was also determined for randomly

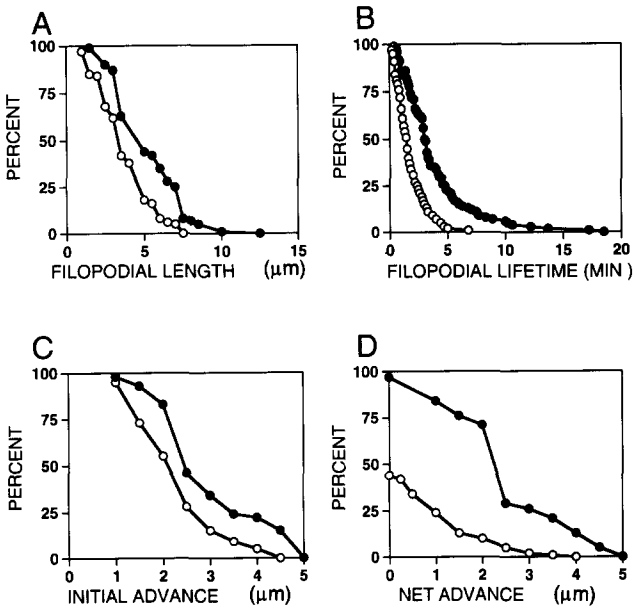

Figure 7. Distribution of combined filopodial lengths (*A*), lifetimes (*B*), and lamellipodial initial (*C*), and net (*D*) advance distances from two control clones and two antisense clones. Primed cells from control and antisense cell lines were plated on a laminin-coated glass coverslip and monitored as described in Fig. 6. Between 5 and 12 filopodia were measured from 5 growth cones each from control clones, D2 and D3, for a total number of 93 filopodia. Between 5 and 10 filopodia were measured from 4 growth cones from clone AS9 and from 9 growth cones from clone AS57 for a total number of 121 filopodia. (*A*) The lengths of individual filopodia are plotted against the percentage of filopodia exceeding that length for control (*closed circles*) and antisense (*open circles*) filopodia. (*B*) The lifetimes of individual filopodia are plotted against the percentage of filopodia exceeding that lifetime for control (*closed circles*) and antisense (*open circles*) filopodia. Between 3 and 5 lamellipodial growth periods were measured from 5 growth cones each from control clones D2 and C3 for a total number of 40 periods. Between 3 and 5 lamellipodial advances were measured from 4 growth cones from clone AS9 and from 9 growth cones from clone AS57 for a total number of 75 periods. (*C*) The distance of individual lamellipodial advance during the advance period is plotted against the percentage of lamellipodia exceeding that distance for control (*closed circles*) and antisense (*open circles*) clones. (*D*) The distance of individual lamellipodial advance during both the advance and quiescent period is plotted against the percentage of lamellipodia exceeding that distance for control (*closed circles*) and antisense (*open circles*) clones.

Table III. Lamellipodial Characteristics

	Advance period	Quiescent period	Initial advance	Net advance
	min	*min*	*μm*	*μm*
Control				
D2 (n = 5)	1.7 ± 0.7	2.5 ± 0.5	3.2 ± 0.7	2.8 ± 0.5
C3 (n = 5)	2.0 ± 1.0	2.2 ± 0.5	3.0 ± 1.1	2.7 ± 0.5
Combined means	1.8 ± 0.8	2.4 ± 0.8	3.1 ± 0.9	2.8 ± 0.5
Vinculin-deficient				
AS9 (n = 4)	1.4 ± 0.4	2.0 ± 0.7	2.4 ± 0.4	0.7 ± 0.2
AS57 (n = 9)	0.9 ± 0.4	1.9 ± 1.1	2.2 ± 0.3	0.6 ± 0.3
Combined means	1.1 ± 0.4	2.0 ± 1.0	2.3 ± 0.3	0.7 ± 0.3
p value	$p < 0.025$	NS*	$p < 0.025$	$p < 0.001$

Lamellipodial characteristics were measured for the same growth cones as those measured in Table II. Periods and distances for each lamellipodial advance from each growth cone was determined. The mean for each respective clone is given (±SEM). A combined mean for the control clones, and a combined mean for the vinculin-deficient clones is given (±SEM). p values were determined using analysis of variance comparing values from the combined clones.
* Not significant.

chosen filopodia. After pooling data, results of the analyses show that filopodia from the antisense clones were slightly shorter than those from the control clones. The mean filopodial length was ~30% less for all the antisense clones compared to the control clones (3.8 vs 5.4 μm). Although small, this difference was significant (Table II). The distribution of filopodial lengths shows that 85–90% of the filopodia from the control and antisense growth cones ranged between 1.6 and 7.5 μm in length (Fig. 7 *A*). Interestingly, very few control filopodia were shorter than 1.6 μm (1%) but there was an abundant number of antisense filopodia this short (15%). Additionally, many of the control filopodia were longer than 6.1 μm (35%), whereas fewer of the antisense filopodia were this long (8%). Therefore, the antisense growth cones seemed to have an abundance of the shortest filopodia and a reduced number of the longest filopodia.

It has been previously observed that longer filopodia have a longer lifetime than shorter filopodia (Aletta and Greene, 1988). We also saw a weak correlation between filopodial length and lifetime in control cells (data not shown). Therefore, it was of interest to determine if the mean filopodial lifetime was different between antisense and controls within a particular class length. For control growth clones, there were 53 filopodia between 4.0 and 6.0 μm in length with a mean lifetime of 5.1 min ± 3.8 min (standard deviation, SD). For the antisense growth cones, there were 52 filopodia which were between 4.0 and 6.0 μm in length with a mean lifetime of 2.2 min ± 1.6 min (SD), ~40% the lifespan of filopodia from growth cones of control PC12 cell clones.

Lamellipodial Dynamics. To determine whether reduced vinculin levels would affect characteristics of lamellipodia, lamellipodia were followed from control and vinculin-deficient growth cones. Lamellipodia from control growth cones flowed onto the substrate, often between two or three filopodial processes (see *white arrow* at 0 s in Fig. 6 *A*), but also were observed growing in the absence of filopodia (see the lamellipodium growing from 288 to 402 s in Fig. 6 *A*). After a period of lamellipodial growth, there was generally a quiescent period when there was no further growth of the lamellipodium (from 180 to 264 s in Fig. 6 *A*). Sometimes, during this quiescent period, a lamellipodium was withdrawn slightly. After this quiescent period, a new lamellipodium generally extended from the same region of the growth cone edge from which the previous lamellipodium had grown, resulting in outgrowth in the same general direction. Rarely, lamellipodia were completely withdrawn and a new lamellipodium initiated from a different region of the growth cone, resulting in outgrowth in a different direction (not shown).

During the advance period, lamellipodia from both vinculin-deficient cells and control cells behaved similarly in that both classes advanced smoothly over the substrate (see from 0 to 150 s in Fig. 6 *A*) and from 0 to 54 s in Fig. 6 *B*). However, during the subsequent quiescent period, lamellipodia from vinculin-deficient cells were often completely

withdrawn back into the growth cone (see 72- 108 s in Fig. 6 *B*). Often lamellipodia were visualized detached from the substratum and waving in the growth medium.

To quantitate behaviors, individual lamellipodia were followed from extension to retraction for each analyzed growth cone as described in the Materials and Methods. During the 20–30 min recording time, there were generally five measurable extensions, although the number ranged from three to eight measurable extensions. For each extension, the following four parameters were quantitated: (*1*) advance period; (*2*) quiescent period; (*3*) distance advanced during advance period (initial advance); and (*4*) total distance advanced during both the advance and quiescent period (net advance). A mean for each parameter was calculated for each growth cone. Four to ten growth cones were followed from each clone and from these means, a mean for the clone was determined (Table III). In control clones, a new lamellipodium grew from the edge of the growth cone on average about every 4–8 min. During the initial growth period which lasted from 20 s to 4 min, a lamellipodium typically flowed forward on average about 3.1 μm. During the quiescent period which lasted from 12 s to 5 min, the lamellipodium did not advance and sometimes retracted slightly. Net advance during the entire period was ~90% of the initial advance so generally a growth cone grew ~2.8 μm with each advance of a lamellipodium (Table III).

Lamellipodia from vinculin-deficient clones were very similar to those from control clones with one major exception. After the period of active growth, there was typically a retraction of much or all of the lamellipodium, so the final net advance was reduced. The advance period, quiescent period, and the initial distance of lamellipodial advance were less in the vinculin-deficient clones compared to the control clones (Table III). For two parameters, the advance period and initial advance distance, the means were significantly reduced, as indicated by the p values. However, these differences were not large (less than 40% reduction, see Table III). The difference between the means for the quiescent period was not statistically significant (Table III). As with the control growth cones, a new lamellipodium grew from vinculin-deficient growth cone edges about every 4–8 min. During the initial growth period which ranged from 10 s to 4 min, a lamellipodium flowed forward on average about 2.3 μm (vs 3.1 min in controls). The distributions for initial advance distance demonstrate that extensions in vinculin-deficient growth cones are generally somewhat less than in controls (Fig. 7 *C*).

In vinculin-deficient cells, the quiescent period lasted an average of 2.0 min (12 s to 5 min), very similar to growth cones of control PC12 cell lines. During this time, most (55%) of the lamellipodia from vinculin-deficient cells were completely retracted. Others were partially retracted. The mean net advance for growth cones from antisense clones AS9 and AS57 was only 20–26% of the initial advance. Hence, the growth cones grew on average only 0.70 and 0.6 μm, respectively, with each lamellipodial advance cycle (Table III), ~25% of that in control PC12 cells. The mean net advance for the vinculin-deficient clones was significantly less than the net advance for the control clones (Table III). The distributions for net advance and initial advance indicate that while the majority of the lamellipodia in vinculin-deficient growth cones are initially extended approximately the same distance as in control lamellipodia, they have a high probability of either completely or partially retracting (compare *open circles*, Fig. 7, *C* and *D*). In marked contrast, most of the control lamellipodia remain extended (compare *closed circles*, Fig. 7, *C* and *D*).

Therefore, the vinculin-deficient growth cones extended surprisingly healthy lamellipodia during the advance period. However, during the quiescent period, the lamellipodia have a high probability of detaching and retracting. This striking reduction of ~70% in net advance of lamellipodia appears sufficient to explain the reduced rates of growth cone advance (~70% reduction, Table III) in vinculin-deficient clones.

Discussion

Localization of Vinculin in PC12 Growth Cones

Several models to explain growth cone migration have been proposed and a critical element of each model is the controlled establishment, maintenance, and subsequent breaking of stable cell-substrate contacts (Mitchison and Kirchner, 1988). Vinculin, a cytoskeletal molecule associated indirectly with integrins and known to be involved in fibroblast adhesion, was an appropriate candidate as a key constituent in the establishment of cell-substrate contacts in neuronal cells.

In growth cones, vinculin was detected in lamellipodia and along the entire length of filopodia. In addition, strong vinculin immunoreactivity was seen in some, but not all, filopodial tips. This is similar to the pattern of β_1 integrin staining in sensory neurons (Letourneau and Shattuck, 1989). Thus it is possible that vinculin mediates substrate contacts at the tip of a subset of filopodia. Interestingly, using interference reflection microscopy, close contacts with the substrate (100-200 A) have been observed at the tips of a subset of filopodia extending from sensory neurons (Letourneau, 1981). Adhesion at the tip of some filopodia has been proposed to explain filopodial buckling observed during outgrowth of mouse cerebral cortex neurons (Sheetz et al., 1992).

Localization of Vinculin and Actin in Vinculin-deficient Cells

To assess the role of vinculin in neuronal outgrowth, vinculin-deficient PC12 cell lines were generated by transfection with retroviral constructs expected to express antisense RNA. This method has proven very useful for defining the role of other cytoskeletal molecules: for example, myosin heavy chain in *Dictyostelium discoideum* (Knect and Loomis, 1987), myosin light chain (Pollenz et al., 1992), α-actinin (Schulze et al., 1989), nonmuscle actin (Izant and Weintraub, 1985), glial fibrillary acidic protein (Weinstein et al., 1991), and most recently, vinculin in fibroblasts (Rodriguez Fernandez et al., 1993).

In nonneuronal cell types, changes in vinculin distribution have been correlated closely with rearrangement of the F-actin cytoskeleton (Tidball and Spencer, 1993). The organization of actin into stress fibers was strikingly dependent on vinculin in some cells (Rodriguez Fernandez et al., 1992, 1993). In many cell types, focal contacts are localized at the end of stress fibers (Heath and Dunn, 1978). Neurons and

neuron-like cell lines do not have readily visible actin stress fibers, and it is therefore difficult to study these structures in neurons. In the present paper, clear differences in F-actin distribution between normal and vinculin-deficient PC12 cells were not seen at this comparatively low level of resolution. These results suggest that localization of actin in growth cones is not sensitive to 5–6-fold reductions in vinculin levels.

Vinculin-deficient PC12 cells seem to attach normally to plastic when growing in cell culture. Also, cell body attachment to laminin is only marginally reduced in vinculin-deficient PC12 cells. Again, since we have reduced vinculin to only 20% of control levels, we cannot conclusively say that vinculin is not involved in cell body attachment to plastic or laminin. In fact, fibroblasts also attached normally when vinculin was reduced to 20% of normal levels with antisense RNA (Rodriguez Fernandez et al., 1993).

Roles of Vinculin and Cell Substrate Contacts in Growth Cone Movements

In this report, we demonstrate that growth cones require a certain level of vinculin for maximal outgrowth. The neurites extended by vinculin-deficient PC12 cell lines were substantially shorter than those extended by control cells. Previous reports have demonstrated that the level of vinculin directly affects the number of cell substrate attachments and hence, the rate of cell motility for fibroblasts. When vinculin was increased in fibroblasts, increased numbers of cell substrate attachments were observed, and a decreased rate of motility was seen (Rodriguez Fernandez et al., 1992). Furthermore, when vinculin was reduced to 20% of normal in fibroblasts, fewer attachments and an increased rate of motility were observed (Rodriguez Fernandez et al., 1993). By immunofluorescence, neurons and neuronal cell lines appear to express lower levels of vinculin compared to more adhesive fibroblasts. Hence, lowering levels in neurons may result in a substantial reduction of substrate attachments within the growth cone so that outgrowth becomes impaired.

To further characterize the phenotype of growth cones expressing reduced levels of vinculin, we used time-lapse video microscopy. In previous work, many growth cone characteristics have been described with some detail. Growth cones migrating on even or patterned substrates in vitro extend filopodia randomly in all directions. All filopodia eventually disappear. Individual filopodia are either retracted or engulfed by an advancing lamellipodium. These latter filopodia seem to provide a structural base for lamellipodial growth. Using video microscopy, we also observed filopodia being extended in almost all directions from PC12 growth cones. These processes were either engulfed by an advancing lamellipodium or were retracted. On average, filopodia were maintained for about 4 min. Aletta and Greene (1988) also observed a similar lifetime for PC12 processes shorter than 10 μm.

Filopodia extending from vinculin-deficient growth cones grew and retracted at the same rate as control filopodia. This result suggests that a vinculin deficiency is unlikely to directly impair the rate of actin filament assembly, since the rate of filopodial extension roughly equals the rate of actin polymerization. However, filopodia from vinculin-deficient growth cones were shorter than control filopodia and more strikingly, vinculin-deficient filopodia had a reduced lifetime of less than 50% compared to control filopodia. Moreover, our results show clearly that vinculin-deficient filopodia of a single length class were maintained for much shorter periods than control filopodia. These results strongly suggest that vinculin is involved in maintaining filopodial extensions. It is possible that the presence of vinculin in cell-substrate contacts at filopodial tips or along the length of filopodia may extend the lifetime of filopodia.

In our cultures, lamellipodia advanced and often seemed to grow between or directly on top of preexisting filopodia. After each advance, there was consistently a period of nongrowth. This quiescent period has been described previously and when measured, was remarkably similar for the PC12 growth cones in this study and for Aplysia growth cones analyzed in another study (Goldberg and Burmeister, 1986). Vinculin-deficient lamellipodia were able to advance almost as far as control lamellipodia and advanced for close to the same amount of time. This suggests that vinculin may not be required for initial lamellipodial growth. However, it is possible that greater reductions in vinculin levels might affect these characteristics. During the quiescent period of a lamellipodial growth cycle, lamellipodia in growth cones of control PC12 cells were stable or retracted slightly. In contrast, most of the lamellipodia from the growth cones of vinculin-deficient cells were completely retracted during the quiescent period, suggesting that vinculin is necessary for lamellipodial stabilization. It appears likely that in the absence of vinculin-containing cell-substrate contacts, lamellipodia are retracted.

Growth cones often follow complex and convoluted pathways in reaching their targets during embryonic development, making many choices between substrates along the way. Due to their dynamics, it is likely that filopodia and lamellipodia are active players in this process. Stabilized attachments by these processes to appropriately localized substrates may help to explain how these choices are made (O'Connor and Bentley, 1993). Since the ability of vinculin to associate with such contacts can be regulated rapidly by receptor tyrosine kinases (Tidball and Spencer, 1993), factors that influence growth cone behavior may act, in part, by regulating levels or interactions of vinculin.

We thank John Sedat, Mel Jones, Hans Chen, and David Sretavan for advice in using the CCD image analysis system. We thank Frances Lefcort and Cristina Weaver for critical reading of the manuscript and Carey Backus for her expert technical assistance. We thank Robert Finney for help in using retroviruses.

This work was supported by US Public Health Service grant NS 19090 to L. F. Reichardt. B. Varnum-Finney was an associate and L. F. Reichardt is an investigator of the Howard Hughes Medical Institute.

Received for publication 30 March 1994 and in revised form 9 August 1994.

References

Aletta, J. M., and L. A. Greene. 1988. Growth cone configuration and advance: a time-lapse study using video-enhanced differential interference contrast microscopy. *J. Neurosci.* 8(4):1425–1435.

Bentley, D., and T. P. O'Connor. 1994. Cytoskeletal events in growth cone steering. *Curr. Opin. Neurobiol.* 4:43–48.

Burridge, K., and P. Mangeat. 1984. An interaction between vinculin and talin. *Nature (Lond.).* 308:744–746.

Chen, H., J. W. Sedat, and D. A. Agard. 1989. Manipulation, display and analysis of three dimensional biological images. *In* The Handbook of Biological Confocal Microscopy. J. Pawley, editor. IMR Press, Madison, WI. 127–135.

Church, G. M., and W. Gilbert. 1984. Genomic sequencing. *Proc. Natl. Acad. Sci. USA.* 81:1991–1995.

Coutu, M. D., and S. W. Craig. 1988. cDNA-derived sequence of chicken embryo vinculin. *Proc. Natl. Acad. Sci. USA.* 85:8535–8539.

Geiger, B. 1979. A 130 K protein from chicken gizzard: its localization at the termini of microfilament bundles in cultured chicken cells. *Cell.* 18: 193–205.

Goldberg, D. J., and D. W. Burmeister. 1986. Stages in axon formation: observations of growth of Aplysia axons in culture using video-enhanced contrast-differential interference contrast microscopy. *J. Cell Biol.* 103:1921–1931.

Gumbiner, B. M. 1993. Proteins associated with the cytoplasmic surface of adhesion molecules. *Neuron.* 11:551–564.

Graham, F. L., and A. J. van der Eb. 1973. A new technique for the assay of infectivity of human adenovirus 5 DNA. *Virology.* 52:456–467.

Heath, J. P., and G. A. Dunn. 1978. Cell to substratum contacts of chick fibroblasts and their relation to the microfilament system. A correlated interference reflection and high-voltage electron microscopic study. *J. Cell Sci.* 21: 129–159.

Halegoua, S. 1987. Changes in the phosphorylation and distribution of vinculin during nerve growth factor induced neurite outgrowth. *Dev. Biol.* 121: 97–104.

Horwitz, A., E. Duggan, C. Buck, M. C. Beckerle, and K. Burridge. 1986. Interaction of plasma membrane fibronectin receptor with talin—a transmembrane linkage. *Nature (Lond.).* 320:531–533.

Hynes, R. O. 1992. Integrins: versatility, modulation, and signaling in cell adhesion. *Cell.* 69:11–25.

Izant, J. G., and H. Weintraub. 1985. Constitutive and conditional suppression of exogenous and endogenous genes by anti-sense RNA. *Science (Wash. DC).* 229:345–352.

Kleinman, H. K., M. L. McGarvey, L. A. Liotta, P. G. Robey, K. Tryggvason, and G. R. Martin. 1982. Isolation and characterization of type IV procollagen, laminin, and heparan sulfate proteoglycan from the EHS sarcoma. *Biochemistry.* 21:6188–6193.

Knecht, D. A., and W. F. Loomis. 1987. Antisense RNA inactivation of myosin heavy chain gene expression in *Dictyostelium discoideum. Science (Wash. DC).* 236:1081–1086.

Laemmli, U. K. 1970. Cleavage of structural proteins during the assembly of the head of bacteriophage T4. *Nature (Lond.).* 227:680–685.

Letourneau, P. C. 1979. Possible roles for cell-to-substratum adhesion in neuronal morphogenesis. *Dev. Biol.* 44:77–91.

Letourneau, P. C. 1983. Differences in the organization of actin in the growth cones compared with the neurites of cultured neurons from chick embryos. *J. Cell Biol.* 97:963–973.

Letourneau, P. C. 1981. Immunocytochemical evidence for colocalization in neurite growth cones of actin and myosin and their relationship for cell-substratum adhesions. *Dev. Biol.* 85:113–122.

Letourneau, P. C., and T. A. Shattuck. 1989. Distribution and possible interactions of actin-associated proteins and cell adhesion molecules of nerve growth cones. *Development.* 105:505–519.

Maniatis, T., E. F. Fritsch, and J. Sambrook. 1989. Molecular Cloning: A Laboratory Manual. 2nd Edition. Cold Spring Harbor Laboratory Press, Cold Spring Harbor, NY. pp 1.1–18.88.

Mann, R., R. Mulligan, and D. Baltimore. 1983. Construction of a retrovirus packaging mutant and its use to produce helper-free defective retrovirus. *Cell.* 33:153–159.

Miller, D. A., and G. J. Rosman. 1989. Improved retroviral factors for gene transfer and expression. *BioTech.* 7:980–990.

Mitchison, T., and M. Kirschner. 1988. Cytoskeletal dynamics and nerve growth. *Neuron.* 1:761–772.

O'Conner, T. P., and D. Bentley. 1993. Accumulation of actin in subsets of pioneer growth cone filopodia in response to neural and epithelial guidance cues in situ. *J. Cell Biol.* 123:935–948.

O'Conner, T. P., J. S. Duerr, and D. Bentley. 1990. Pioneer growth cone steering decisions mediated by single filopodial contacts in situ. *J. Neurosci.* 10:3935–3946.

Otey, C. A., F. M. Pavalko, and K. Burridge. 1990. An interaction between α-actinin and the β_1 integrin subunit in vitro. *J. Cell Biol.* 111:721–729.

Pollenz, R. S., T.-L. L. Chen, L. Trivinos-Lagos, and R. L. Chisholm. 1992. The *Dictyostelium* essential light chain is required for myosin function. *Cell.* 69:951–962.

Rodriguez Fernandez, J. L., B. Geiger, D. Salomon, and A. Ben-Ze'ev. 1992. Overexpression of vinculin suppresses motility in BALB/c 3T3 cells. *Cell Motil. Cytoskeleton.* 22:127–134.

Rodriguez Fernandez, J. L., B. Geiger, D. Salomon, I. Sabanay, M. Zoller, and A. Ben-Ze'ev. 1992. Suppression of tumorigenicity in transformed cells after transfection with vinculin cDNA. *J. Cell Biol.* 119:427–438.

Rodriguez Fernandez, J. L., B. Geiger, D. Salomon, and A. Ben-Ze'ev. 1993. Suppression of vinculin expression by antisense transfection confers changes in cell morphology, motility, and anchorage-dependent growth of 3T3 cells. *J. Cell Biol.* 122(6):1285–1294.

Schulze, H., A. Huchriede, A. A. Noegel, M. Schleicher, and B. M. Jockush. 1989. Alpha-actinin synthesis can be modulated by antisense probes and is autoregulated in non-muscle cells. *EMBO (Eur. Mol. Biol. Organ.) J.* 8:3587–3593.

Sheetz, M. P., D. B. Wayne, and A. L. Pearlman. 1992. Extension of filopodia by motor-dependent actin assembly. *Cell Motil. Cytoskeleton.* 22:160–169.

Sokol, R. R., and F. J. Rohlf. 1969. Biometry. W. H. Freeman and Co., San Francisco, CA. pp 204–252.

Tidball, J. G., and M. J. Spencer. 1993. PDGF stimulation induces phosphorylation of talin and cytoskeletal reorganization in skeletal muscle. *J. Cell Biol.* 123:627–635.

Timpl, R., H. Rohdl, L. Ristidi, Au Ott, P. G. Riber, and G. R. Martin. 1982. Laminin. *Methods Enzymol.* 82:831–838.

Tomaselli, K. J., D. E. Hall, L. A. Flier, K. R. Gehlsen, D. C. Turner, S. Carbonetto, and L. F. Reichardt. 1990. A neuronal cell line (PC12) expresses two β1-class integrins—$\alpha 1\beta 1$ and $\alpha 3\beta 1$—that recognize different neurite outgrowth-promoting domains in laminin. *Neuron.* 5:651–662.

Tomaselli, K. J., C. H. Damsky, and L. F. Reichardt. 1987. Interactions of a neuronal cell line (PC12) with laminin, collagen IV and fibronectin: identification of integrin-related glycoproteins involved in attachment and process outgrowth. *J. Cell Biol.* 105:2347–2358.

Weinstein, D. E., M. Shelanski, and F. K. H. Liem. 1991. Suppression by antisense mRNA demonstrates a requirement for the glial fibrillary acidic protein in the formation of stable astrocytic processes in response to neurons. *J. Cell Biol.* 112:1205–1213.

Wachsstock, D. H., J. A. Wilkins, and S. Lin. 1987. Specific interaction of vinculin with alpha-actinin. *Biochem. Biophys. Res. Commun.* 146:554–560.